Available online at www.sciencedirect.com
SCIENCE DIRECT®
Journal of Sound and Vibration 283 (2005) 1216–1228
JOURNAL OF SOUND AND VIBRATION
www.elsevier.com/locate/jsvi

Short Communication

Analysis of buckled and pre-bent fixed-end columns used as vibration isolators

R.H. Plaut[a,*], J.E. Sidbury[a], L.N. Virgin[b]

[a]*Department of Civil and Environmental Engineering, Virginia Polytechnic Institute and State University, Blacksburg, VA 24061-0105, USA*
[b]*Department of Mechanical Engineering and Materials Science, Duke University, Durham, NC 27708-0300, USA*

Received 19 February 2004; received in revised form 18 June 2004; accepted 19 July 2004
Available online 16 December 2004

Abstract

The use of a buckled or pre-bent column with fixed ends as a vibration isolator is analyzed. The column is designed to have a high axial stiffness under the weight that it supports, so that the static displacement of the weight is not excessive, and then to have a low stiffness during excitation. The base of the column is assumed to have an axial motion which is simple harmonic or a linear combination of two simple harmonic functions. The column is modeled as an elastica. First the equilibrium shape under the supported weight is determined. Then small steady-state vibrations about the equilibrium configuration are obtained numerically using a shooting method. The inertia of the supported weight and the transverse and axial inertias of the column are included. The axial displacement transmissibility is computed, and the effects of external and internal damping, column stiffness, supported weight, and initial curvature are investigated. For the two-frequency excitation, the effects of the relative amplitudes and frequencies of the excitation components are considered.

1. Introduction

Isolators are placed between a ''base'' and a ''system'', either to reduce the transmission of motions from the system to the base, or to reduce the effect of base motions on the system [1].

*Corresponding author. Tel.: +1 540 231 6072; fax: +1 540 231 7532.
E-mail address: rplaut@vt.edu (R.H. Plaut).

0022-460X/$ - see front matter © 2004 Elsevier Ltd. All rights reserved.
doi:10.1016/j.jsv.2004.07.029

Effective filtering often requires that the dominant excitation frequency be higher than the fundamental frequency of the system. Therefore, it is desirable that this latter frequency be low. Sometimes it is also required that the static deflection of the weight supported by the isolator be small (e.g., if there is a displacement constraint). Slightly buckled or pre-bent columns may be useful in satisfying these two characteristics.

Winterflood et al. [2–4] discussed such a potential application of buckled columns with fixed ends. They performed a static analysis, conducted static and vibration tests, and obtained transfer functions. Virgin and Davis [5] carried out experiments involving a weight supported by two buckled pinned–pinned columns in parallel. Vertical harmonic base excitation was applied, and the vertical response of the weight was measured. A similar type of isolator consisting of a buckled mechanism (two rigid bars with a rotational spring at the connecting hinge) was analyzed by Plaut et al. [6]. Both parametric and external (forcing) excitations appeared in the equation of motion, and chaotic responses were exhibited for certain large base motions.

The related problem of free vibrations of buckled columns has been studied in a number of papers. Virgin [7] performed a one-mode analysis for a pinned–pinned column, Nayfeh et al. [8] treated fixed–fixed, fixed–pinned, and pinned–pinned columns (with the assumption that the equilibrium shape along the post-buckling path is the same as at the origin of that path), and Lestari and Hanagud [9] considered columns with rotational springs at the ends. In the field of nanomechanics, Nicu and Bertaud [10] and Nicu et al. [11] conducted experiments on buckled fixed–fixed ''microbridges''.

The response of buckled columns to harmonic axial loading was investigated by Abou-Rayan et al. [12] and Ji and Hansen [13]. Since the column is not straight, parametric and external excitations are involved in the analysis. In Ref. [12], the same approximation as in Ref. [8] was made and large responses were computed for a pinned–pinned column. In Ref. [13], experiments were carried out on fixed–fixed columns.

Here the dynamic response is analyzed for a buckled or pre-bent fixed–fixed column that supports a weight and is subjected to axial motion at its base. It is assumed that horizontal motion of the supported weight is suppressed, without affecting the vertical motion. Section 2 contains the formulation for the case of simple harmonic base motion, and results are presented in Section 3. Excitation consisting of a linear combination of two harmonic motions is considered in Section 4, and concluding remarks are given in Section 5.

2. Formulation for simple harmonic excitation

The column is assumed to be an elastica, which is thin, flexible, inextensible, and unshearable [14]. It is uniform with constant bending stiffness EI, constant mass per unit length μ, and length L. The supported weight at the top of the column is P_0, and the weight of the column is neglected. From the base, the arc length is S, the axial and transverse coordinates are $X(S,T)$ and $Y(S,T)$, respectively, and the rotation angle in radians is $\theta(S,T)$, where T denotes time. The column is unstrained when the rotation angle is $\theta_0(S)$, with $\theta_0(0)=\theta_0(L)=0$. The coefficients of external and internal (Kelvin–Voigt) damping are C and Γ, respectively. The bending moment $M(S,T)$ is

given by [15]

$$M = EI\left(\frac{\partial\theta}{\partial S} - \frac{\mathrm{d}\theta_0}{\mathrm{d}S}\right) + \Gamma I \frac{\partial}{\partial T}\left(\frac{\partial\theta}{\partial S}\right). \tag{1}$$

The axial and transverse forces in the column are denoted $P(S,T)$ and $Q(S,T)$, respectively, $U(T)$ is the axial displacement of the base with U_0 being its amplitude, and Ω is an applied frequency. The analysis is carried out in terms of the nondimensional quantities

$$\begin{aligned} &x = \frac{X}{L}, \quad y = \frac{Y}{L}, \quad s = \frac{S}{L}, \quad u = \frac{U}{L}, \quad u_0 = \frac{U_0}{L}, \\ &m = \frac{ML}{EI}, \quad p_0 = \frac{P_0 L^2}{EI}, \quad p = \frac{PL^2}{EI}, \quad q = \frac{QL^2}{EI}, \quad r = \frac{EI}{\mu g L^3}, \\ &c = \frac{CL^2}{\sqrt{\mu EI}}, \quad \gamma = \frac{\Gamma\sqrt{I}}{\sqrt{\mu E L^4}}, \quad t = T\sqrt{\frac{EI}{\mu L^4}}, \quad \omega = \Omega\sqrt{\frac{\mu L^4}{EI}}, \end{aligned} \tag{2}$$

where r will be called the stiffness parameter.

In nondimensional terms, the column is drawn in a horizontal configuration in Fig. 1, with its base at the left. A free body diagram of an element of the column is depicted in Fig. 2. Based on geometry, Eq. (1), and dynamic equilibrium in Fig. 2, the governing nondimensional equations are as follows:

$$\begin{aligned} &\frac{\partial x}{\partial s} = \cos\theta, \quad \frac{\partial y}{\partial s} = \sin\theta, \quad \frac{\partial\theta}{\partial s} - \frac{\mathrm{d}\theta_0}{\mathrm{d}s} + \gamma\frac{\partial^2\theta}{\partial t\partial s} = m, \\ &\frac{\partial m}{\partial s} = -p\sin\theta + q\cos\theta, \quad \frac{\partial p}{\partial s} = -\frac{\partial^2 x}{\partial t^2} - c\frac{\partial x}{\partial t}, \quad \frac{\partial q}{\partial s} = -\frac{\partial^2 y}{\partial t^2} - c\frac{\partial y}{\partial t}. \end{aligned} \tag{3}$$

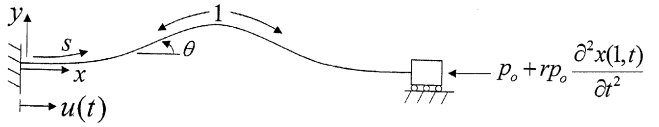

Fig. 1. Geometry of buckled or pre-bent column subjected to base motion and to static and inertia forces of supported weight, in nondimensional terms.

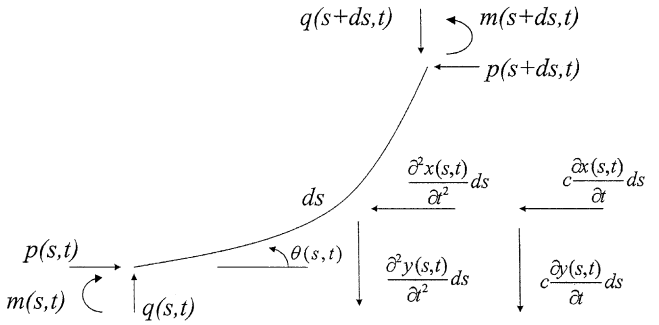

Fig. 2. Free body diagram of column element, including inertia and external damping forces.

The boundary conditions at $s = 0$ are

$$x(0,t) = u(t), \quad y(0,t) = 0, \quad \theta(0,t) = 0. \tag{4}$$

At $s = 1$, the boundary conditions are

$$y(1,t) = 0, \quad \theta(1,t) = 0, \quad p(1,t) = p_0 + rp_0 \frac{\partial^2 x(1,t)}{\partial t^2}. \tag{5}$$

For simple harmonic axial base excitation, it is assumed that

$$u(t) = u_0 e^{i\omega t}, \tag{6}$$

where $u_0 > 0$.

First the equilibrium configuration is analyzed. The subscript "e" is used for the corresponding quantities. The internal forces are $p_e = p_0$ and $q_e = 0$, and the governing equations for the remaining quantities are

$$\frac{dx_e}{ds} = \cos\theta_e, \quad \frac{dy_e}{ds} = \sin\theta_e, \quad \frac{d\theta_e}{ds} = m_e + \frac{d\theta_0}{ds}, \quad \frac{dm_e}{ds} = -p_0 \sin\theta_e. \tag{7}$$

The boundary conditions are $x_e(0) = 0, y_e(0) = 0, \theta_e(0) = 0, y_e(1) = 0$ and $\theta_e(1) = 0$. Eqs. (7) are solved numerically using a shooting method with the subroutines NDSolve and FindRoot in Mathematica [16]. For given supported weight p_0 and initial displacement $\theta_0(s)$, the value of $m_e(0)$ is varied until one of the boundary conditions at $s = 1$ is satisfied with sufficient accuracy [17].

Next, small steady-state vibrations about the equilibrium configuration are considered. The variables are written in the following complex form:

$$\begin{aligned} &x(s,t) = x_e(s) + x_d(s)e^{i\omega t}, \quad y(s,t) = y_e(s) + y_d(s)e^{i\omega t}, \\ &\theta(s,t) = \theta_e(s) + \theta_d(s)e^{i\omega t}, \quad m(s,t) = m_e(s) + m_d(s)e^{i\omega t}, \\ &p(s,t) = p_0 + p_d(s)e^{i\omega t}, \quad q(s,t) = q_d(s)e^{i\omega t}, \end{aligned} \tag{8}$$

where the subscript "d" designates "dynamic". The dynamic quantities are assumed to be small, and the resulting linear equations for these quantities are as follows:

$$\begin{aligned} &\frac{dx_d}{ds} = -\theta_d \sin\theta_e, \quad \frac{dy_d}{ds} = \theta_d \cos\theta_e, \quad \frac{d\theta_d}{ds} = \frac{m_d}{(1 + i\omega\gamma)}, \\ &\frac{dm_d}{ds} = (q_d - p_0\theta_d)\cos\theta_e - p_d \sin\theta_e, \quad \frac{dp_d}{ds} = (\omega^2 - i\omega c)x_d, \\ &\frac{dq_d}{ds} = (\omega^2 - i\omega c)y_d. \end{aligned} \tag{9}$$

The boundary conditions are $x_d(0) = u_0, y_d(0) = 0, \theta_d(0) = 0, y_d(1) = 0, \theta_d(1) = 0$, and $p_d(1) = -rp_0\omega^2 x_d(1)$.

The solution procedure for Eqs. (9) is similar to that for equilibrium. The weight p_0, initial rotation angle $\theta_0(s)$, external damping coefficient c, internal damping coefficient γ, stiffness parameter r, excitation amplitude u_0, and excitation frequency ω are specified, and $m_e(0)$ is known from the equilibrium solution. The quantities $m_d(0), p_d(0)$, and $q_d(0)$ are varied until the boundary conditions at $s = 1$ are satisfied [17].

The transmissibility TR is defined as the ratio of the amplitude of the axial motion of the supported weight to the amplitude of the applied axial motion at the base of the column. Hence,

$$\mathrm{TR} = \frac{\sqrt{\{\mathrm{Re}[x_d(1)]\}^2 + \{\mathrm{Im}[x_d(1)]\}^2}}{u_0} \tag{10}$$

and TR is independent of u_0 (since x_d is proportional to u_0). The objective is for TR to be much less than unity for a large range of excitation frequencies, or at least for the expected range to which the system will be subjected.

In some of the numerical examples, the column will be "perfect", i.e., unstrained when straight ($\theta_0(s) = 0$), and the supported weight will be slightly above the critical load $p_{\mathrm{CR}} = 4\pi^2 = 39.48$. In the remaining examples, the column will have an initial displacement (before supporting the weight p_0) in the shape of the first buckling mode, i.e.,

$$\theta_0(s) = a_0 \sin 2\pi s, \tag{11}$$

in which case the corresponding central displacement is $y = 0.32a_0$.

3. Results for simple harmonic excitation

First the column is assumed to be perfect, i.e., $a_0 = 0$. In most of the figures, the transmissibility TR will be plotted as a function of the excitation frequency ω. For sufficiently small damping and sufficiently high values of the stiffness parameter r, the curves have an infinite number of peaks, usually diminishing in magnitude as the frequency increases. Only the first peak will be included in the frequency range used in many of the figures, and the corresponding frequency will be called the peak frequency.

In Fig. 3, the abscissa is $\omega\sqrt{r}$ rather than ω to show the effect of the column bending stiffness EI on the transmissibility. Since the definition of the nondimensional frequency ω depends on EI, the abscissa in Fig. 3 is chosen to be proportional to the dimensional applied frequency. For $p_0 = 40$, $c = 1$, and $\gamma = 0$, transmissibility curves are shown for stiffness parameter values $r = 0.1, 1$, and

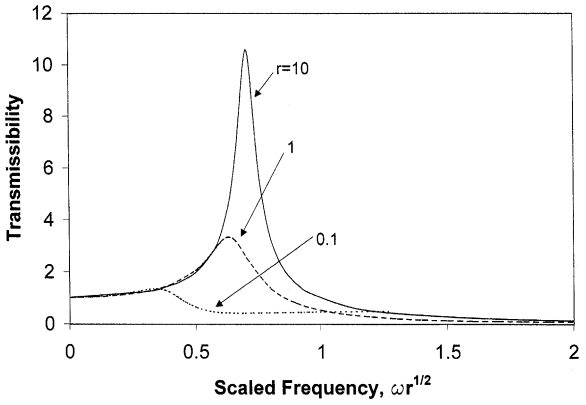

Fig. 3. Variation of transmissibility with $\omega\sqrt{r}$ (proportional to dimensional frequency); $p_0 = 40, c = 1, \gamma = 0, a_0 = 0$. ·····, $r = 0.1$; - - - -, $r = 1$; ——, $r = 10$.

10. It is seen that the peak dimensional frequency increases as the column bending stiffness increases. Also, the maximum value of the transmissibility increases, as shown explicitly in Fig. 4 for this weight $p_0 = 40$ and also for $p_0 = 41$ (again with $c = 1$ and $\gamma = 0$).

Fig. 5 illustrates the effect of internal damping for the case $p_0 = 40, r = 0.1$, and $c = 0$. The external damping coefficient c has a similar influence on the transmissibility curves [17]. The effect of the supported weight is shown in Fig. 6, where $r = 1, c = 1$, and $\gamma = 0$. The central transverse displacement of the column in equilibrium under the weight is $y = 0.10$ for $p_0 = 40$ and $y = 0.17$ for $p_0 = 41$. An increase in the weight from $p_0 = 40$ to 41 causes a significant increase in the maximum transmissibility (also see Fig. 4) and a small increase in the peak frequency.

Next, the column is assumed to be pre-bent with its initial rotation angle given by Eq. (11). Cases of supported weight less than the critical load are included in the numerical results. First the equilibrium configuration is determined, and Table 1 lists the central deflection $y_e(0.5)$ and the end

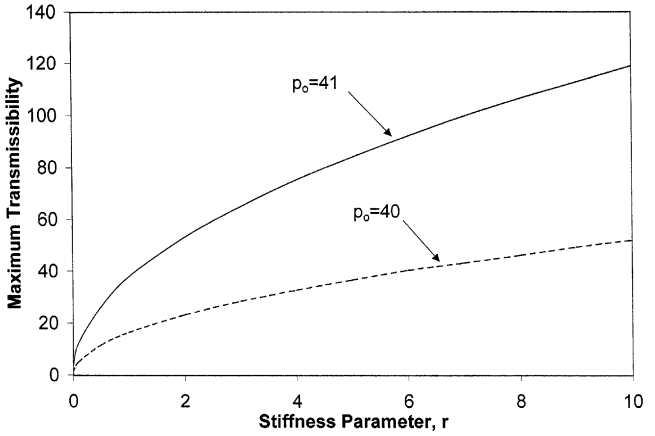

Fig. 4. Maximum transmissibility vs. stiffness parameter; $c = 1, \gamma = 0, a_0 = 0$. ----, $p_0 = 40$; ——, $p_0 = 41$.

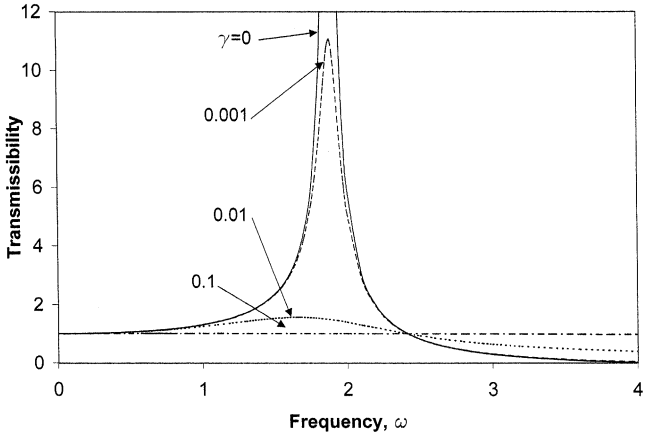

Fig. 5. Transmissibility curves; $p_0 = 40, r = 0.1, c = 0, a_0 = 0$. ——, $\gamma = 0$; ----, $\gamma = 0.001$; ⋯, $\gamma = 0.01$; —·—, $\gamma = 0.1$.

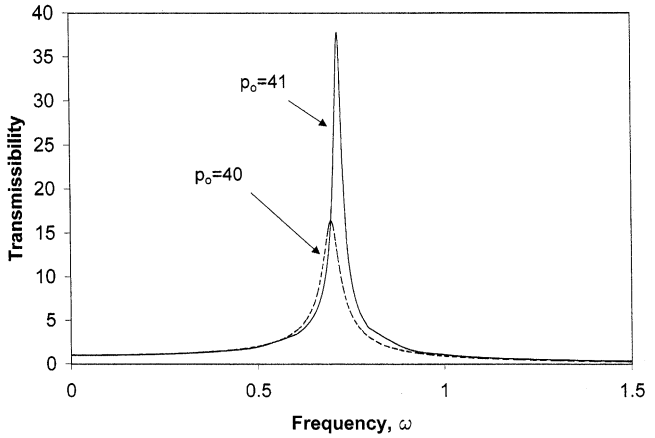

Fig. 6. Transmissibility curves; $r = 1, c = 1, \gamma = 0, a_0 = 0$. ----, $p_0 = 40$; ——, $p_0 = 41$.

Table 1
Central displacement and end shortening for various supported weights, in nondimensional terms

$a_0 = 0.05$			$a_0 = 0.05$			$a_0 = 0.10$		
p_0	$y_e(0.5)$	δ	p_0	$y_e(0.5)$	δ	p_0	$y_e(0.5)$	δ
10	0.0043	0.000045	10	0.021	0.00050	10	0.043	0.0020
20	0.0064	0.00010	20	0.032	0.0019	20	0.064	0.0076
30	0.013	0.00043	30	0.065	0.0098	30	0.12	0.036
40	0.16	0.064	40	0.23	0.15	40	0.28	0.22

shortening δ for weights $p_0 = 10$, 20, 30, and 40, with $a_0 = 0.01$, 0.05, and 0.10. Transmissibility curves are plotted in Fig. 7 for $p_0 = 40$ and in Fig. 8 for $p_0 = 10$ (with $r = 1$, $c = 1$, and $\gamma = 0$). In Fig. 7, as a_0 increases, the peak frequency and maximum transmissibility increase. For the case $p_0 = 10$ in Fig. 8, however, the peak frequency decreases as a_0 increases (see Fig. 9). No curve is shown for the perfect column, since it does not exhibit transverse motion when $p_0 < p_{CR}$.

To be effective as an isolator, the transmissibility TR should be less than unity. In Fig. 7, the range in which this occurs (which lies to the right of the peak and after TR decreases below unity) becomes smaller as a_0 increases. Therefore, if the supported weight will be greater than the critical load, the unstrained column should be as straight as possible.

To illustrate the behavior when the applied frequency is higher than plotted in the previous figures, transmissibility curves for a larger frequency range, $0 < \omega < 300$, are depicted in Figs. 10 and 11. The parameters are $a_0 = 0.05$, $r = 1$, $c = 0.1$, and $\gamma = 0$. In Fig. 10, the transmissibility is plotted up to TR = 20 and curves for $p_0 = 10$, 20, 30, and 40 are presented, whereas the range is $0 < \text{TR} < 2$ in Fig. 11 and only curves for $p_0 = 20$ and 40 are shown. For $p_0 = 40$, the five peaks occur at $\omega = 0.88$, 45, 77, 142, and 227. The corresponding vibration modes about the equilibrium configuration have zero, one, two, three, and four nodes, respectively, and are alternately symmetric and anti-symmetric about the center $s = 0.5$ [17]. If $p_0 < p_{CR}$, the local transmissibility peaks corresponding to the anti-symmetric modes are very small, as seen at $\omega = 54$ and 190 in Fig. 11.

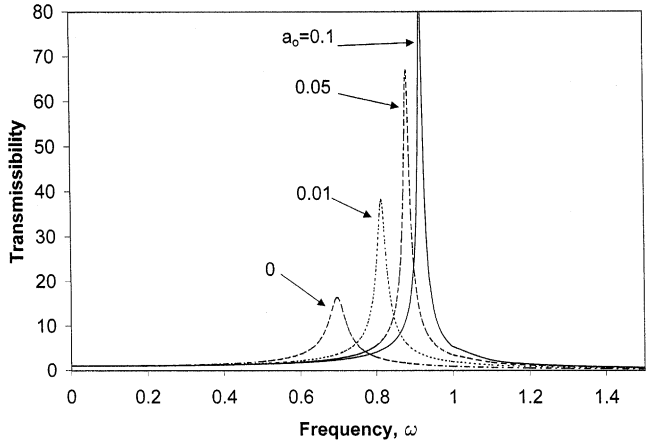

Fig. 7. Transmissibility curves; $p_0 = 40, r = 1, c = 1, \gamma = 0$. ----, $a_0 = 0$; $\cdots$, $a_0 = 0.01$; ——, $a_0 = 0.05$; ——, $a_0 = 0.1$.

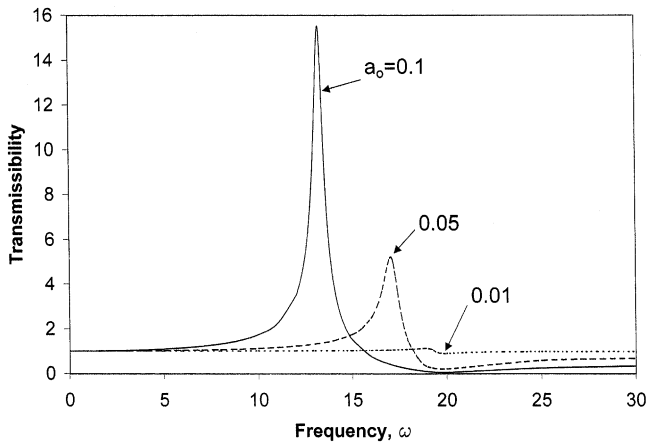

Fig. 8. Transmissibility curves; $p_0 = 10, r = 1, c = 1, \gamma = 0$. $\cdots$, $a_0 = 0.01$; ----, $a_0 = 0.05$; ——, $a_0 = 0.1$.

With regard to the effectiveness of the column as an isolator, Fig. 11 indicates that the transmissibility is almost zero for large ranges of applied frequency if the weight is slightly above the critical load for this imperfect case. For weights lower than the critical load, the frequency ranges in which the transmissibility is very low are not as large.

4. Two-frequency excitation

In this section, the axial excitation is assumed to have the form

$$u(t) = u_0 e^{i\omega t} + r_a u_0 e^{ir_f \omega t}, \tag{12}$$

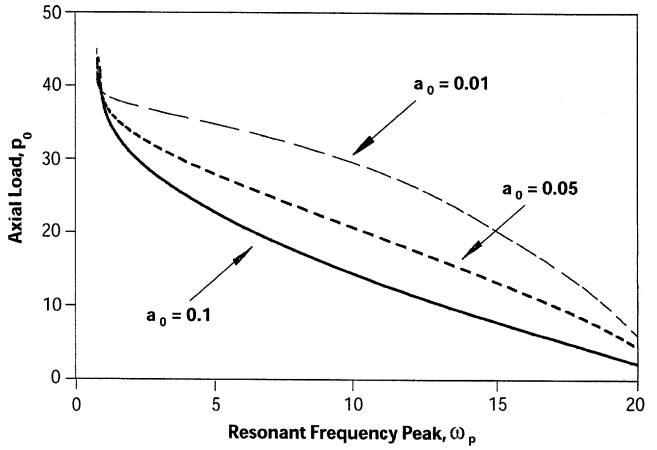

Fig. 9. Weight vs. peak frequency; $r = 1, c = 1, \gamma = 0$. ——, $a_0 = 0.01$; ----, $a_0 = 0.05$; ——, $a_0 = 0.1$.

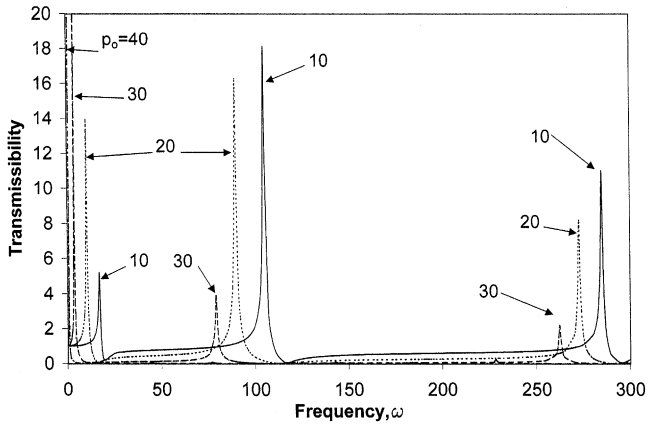

Fig. 10. Transmissibility curves with $0 < \omega < 300; r = 1, c = 0.1, \gamma = 0, a_0 = 0.05$. ——, $p_0 = 10$; ----, $p_0 = 20$; ——, $p_0 = 30$; —·—, $p_0 = 40$.

where $u_0 > 0$, $r_a > 0$, and $r_f > 1$, with r_a and r_f representing the ratios of the amplitude and frequency, respectively, of the added component to those of the original one. The analysis is similar to that for the single-frequency excitation, but the steady-state vibrations have two dynamic components. For example,

$$x(s,t) = x_e(s) + x_1(s)e^{i\omega t} + x_2(s)e^{ir_f\omega t}. \tag{13}$$

Eqs. (9) are replaced by two similar sets of six equations. It is assumed that there is no initial displacement of the column ($a_0 = 0$).

For a given excitation (12), the axial response $x(1,t)$ of the weight is not simple harmonic motion and is not proportional to the axial base excitation. The transmissibility is defined in a different way than previously. The dynamic axial response, given by the real part of the last two terms in Eq. (13) at $s = 1$, is computed for a length of time equal to 50 periods of the second

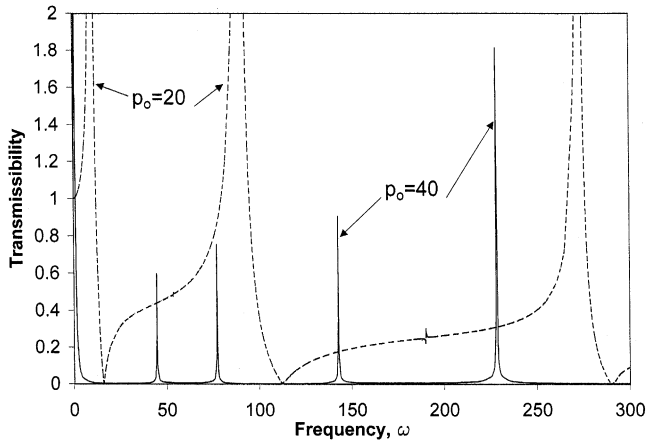

Fig. 11. Transmissibility curves with $0<\omega<300$ and $0<\mathrm{TR}<2; r=1, c=0.1, \gamma=0, a_0=0.05$. ----, $p_0=20$; ——, $p_0=40$.

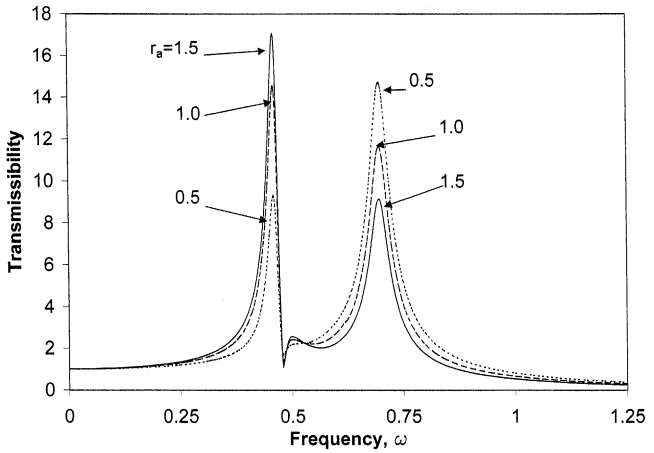

Fig. 12. Transmissibility curves; $p_0=40, r=1, c=1, \gamma=0, a_0=0, r_f=1.5$. $\cdots\cdots$, $r_a=0.5$; ----, $r_a=1.0$; ——, $r_a=1.5$.

dynamic component. The root mean square of this response is used as the numerator of the transmissibility ratio, and the root mean square of the real part of Eq. (12) over the same range of time is used as the denominator.

Fig. 12 shows the effect of the amplitude ratio r_a for the case $p_0=40$, $r=1$, $c=1$, $\gamma=0$, and frequency ratio $r_f=1.5$, for the range $0<\omega<1.25$. The second component of excitation causes a second peak at a value of ω approximately equal to $\frac{2}{3}$ of the original peak frequency. The relative heights of the peaks depend on r_a, with the first peak being higher if r_a is sufficiently large. For higher modes, the second component in Eq. (12) also causes additional peaks to occur at frequencies approximately $\frac{2}{3}$ of those of the peaks due to the first component. These additional peaks reduce the regions of frequencies in which the column is an effective isolator, compared to the single-frequency case.

The effect of the bending stiffness of the column is depicted in Fig. 13. As in Fig. 3, the abscissa is $\omega\sqrt{r}$ rather than ω. In Fig. 13, $p_0 = 40, c = 1, \gamma = 0$, the amplitude ratio is $r_a = 1$, and the frequency ratio is $r_f = 2$. The transmissibility is only plotted to a value of 2. Stiffness parameter values $r = 0.1$, 1, and 10 are considered. For each r, the first peak is at half the frequency of the second peak. The curve for $r = 0.1$ dips down to a low value of transmissibility at a lower value of the dimensional frequency than for the cases $r = 1$ and 10.

Finally, Fig. 14 illustrates the effect of the second component of the excitation. For both curves, $p_0 = 40$, $r = 0.1$, $c = 1$, and $\gamma = 0$. The solid curve corresponds to a single-frequency excitation. For the dashed curve, the amplitude ratio is 1 and the frequency ratio is 2. With respect to an

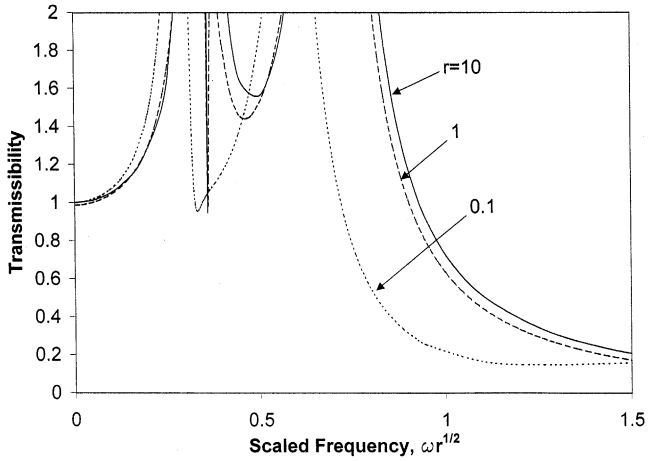

Fig. 13. Variation of transmissibility with $\omega\sqrt{r}$ (proportional to dimensional frequency); $p_0 = 40, c = 1, \gamma = 0, a_0 = 0, r_a = 1, r_f = 2$. $\cdots$, $r = 0.1$; ----, $r = 1$; ——, $r = 10$.

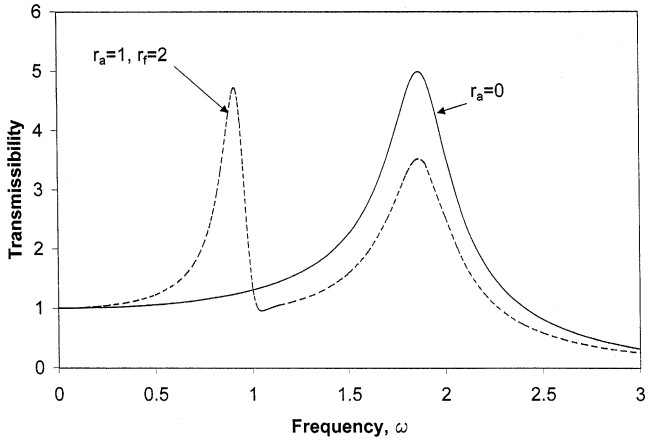

Fig. 14. Transmissibility curves; $p_0 = 40, r = 0.1, c = 1, \gamma = 0, a_0 = 0$. —— $r_a = 0$ (single-frequency excitation); ---- $r_a = 1$ and $r_f = 2$ (two-frequency excitation).

application as an isolator, for $0<\omega<3$ in Fig. 14 the transmissibility is less than unity for a larger range of frequencies when the input includes the second component.

5. Concluding remarks

The application of a slightly-buckled or slightly-bent fixed–fixed column as an isolator was analyzed. Small axial base excitations were considered, consisting of one or two simple harmonic components. The transmissibility was defined as a ratio of amplitude measures of the motions of the supported weight and the base, and the objective is for this ratio to be much less than unity. In practice, a rigid or flexible body could be supported by a number of such columns.

The column was modeled as an inextensible elastica, which allows large displacements in equilibrium. Also, this model makes it easy to include both transverse and axial inertia forces of the column in the governing equations, and to include the base displacement excitation and the axial inertia force of the supported weight as boundary conditions. Numerical solutions were obtained with the use of a shooting method, in which the boundary value problem was treated as an initial value problem. First the equilibrium configuration was obtained, and then small steady-state vibrations about this configuration were analyzed.

For sufficiently low damping and sufficiently high column stiffness, the transmissibility curves exhibit an infinite number of peaks. Considering harmonic base motion, for columns with no initial displacement, it is advantageous for the weight to be only slightly above the critical load. For columns with initial displacement in the shape of the first buckling mode, lower transmissibilities are exhibited between the peaks if the supported weight is above the critical load. If the weight is lower than the critical load, the transmissibility peaks corresponding to anti-symmetric modes are very small.

Considering the addition of a second harmonic component of base motion which has a higher frequency than the first, another set of transmissibility peaks occurs at correspondingly lower frequencies. In the examples treated, the transmissibility in frequency ranges between the peaks is almost the same as if the excitation only contained the first frequency.

Buckled or pre-bent columns have the potential to act as effective vibration isolators which can support weights without significant vertical deflections, and possess low fundamental frequencies which could lead to low transmissibilities for large ranges of applied frequencies.

Acknowledgements

This research was supported by the US National Science Foundation under Grant No. CMS-0301084. The authors are grateful to the reviewers for their helpful comments.

References

[1] E.I. Rivin, *Passive Vibration Isolation*, ASME Press, New York, 2003.

[2] J. Winterflood, T. Barber, D.G. Blair, Using Euler buckling springs for vibration isolation, *Classical and Quantum Gravity* 19 (2002) 1639–1645.
[3] J. Winterflood, D.G. Blair, B. Slagmolen, High performance vibration isolation using springs in Euler column buckling mode, *Physics Letters A* 300 (2002) 122–130.
[4] J. Winterflood, T.A. Barber, D.G. Blair, Mathematical analysis of an Euler spring vibration isolator, *Physics Letters A* 300 (2002) 131–139.
[5] L.N. Virgin, R.B. Davis, Vibration isolation using buckled struts, *Journal of Sound and Vibration* 260 (2003) 965–973.
[6] R.H. Plaut, L.A. Alloway, L.N. Virgin, Nonlinear oscillations of a buckled mechanism used as a vibration isolator, *Proceedings of the IUTAM Symposium on Chaotic Dynamics and Control of Systems and Processes in Mechanics*, Rome, Italy, May 2003.
[7] L.N. Virgin, The dynamics of symmetric post-buckling, *International Journal of Mechanical Sciences* 27 (1985) 235–248.
[8] A.H. Nayfeh, W. Kreider, T.J. Anderson, Investigation of natural frequencies and mode shapes of buckled beams, *AIAA Journal* 33 (1995) 1121–1126.
[9] W. Lestari, S. Hanagud, Nonlinear vibration of buckled beams: some exact solutions, *International Journal of Solids and Structures* 38 (2001) 4741–4757.
[10] L. Nicu, C. Bergaud, Experimental and theoretical investigations on nonlinear resonances of composite buckled microbridges, *Journal of Applied Physics* 86 (1999) 5835–5840.
[11] L. Nicu, P. Temple-Boyer, C. Bergaud, E. Scheid, A. Martinez, Energy study of buckled micromachined beams for thin-film stress measurements applied to SiO_2, *Journal of Micromechanics and Microengineering* 9 (1999) 414–421.
[12] A.M. Abou-Rayan, A.H. Nayfeh, D.T. Mook, M.A. Nayfeh, Nonlinear response of a parametrically excited buckled beam, *Nonlinear Dynamics* 4 (1993) 499–525.
[13] J.-C. Ji, C.H. Hansen, Non-linear response of a post-buckled beam subjected to a harmonic axial excitation, *Journal of Sound and Vibration* 237 (2000) 303–318.
[14] E.M. Mockensturm, J. Jiang, Active structures using buckling beam actuators, *Proceedings of the 44th AIAA/ASME/ASCE/AHS Structures, Structural Dynamics, and Materials Conference*, Norfolk, VA, April 2003.
[15] R.W. Clough, J. Penzien, *Dynamics of Structures*, second ed., McGraw-Hill, New York, 1993.
[16] S. Wolfram, *The Mathematica Book*, third ed., Cambridge University Press, Cambridge, UK, 1996.
[17] J.E. Sidbury, Analysis of Buckled and Pre-bent Columns Used as Vibration Isolators, MS Thesis, Virginia Polytechnic Institute and State University, Blacksburg, VA, 2003.